

## Supporting Information

### Controlled Synthesis of Concave $\text{Cu}_2\text{O}$ Microcrystals Enclosed by $\{hhl\}$ High-index Facets and Enhanced Catalytic Activity†

Xue Wang, Chang Liu, Binjie Zheng, Yaqi Jiang, Lei Zhang, Zhaoxiong Xie\* and Lansun Zheng

State Key Laboratory for Physical Chemistry of Solid Surfaces & Department of Chemistry,  
College of Chemistry and Chemical Engineering, Xiamen University, Xiamen 361005, China.

E-mail: zxxie@xmu.edu.cn

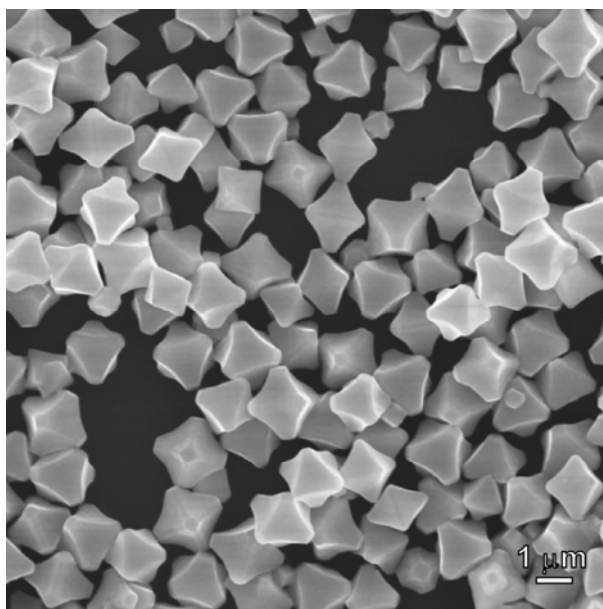


**Fig. S1** The SEM image of truncated concave octahedral  $\text{Cu}_2\text{O}$  microcrystals with 5 mM glucose.

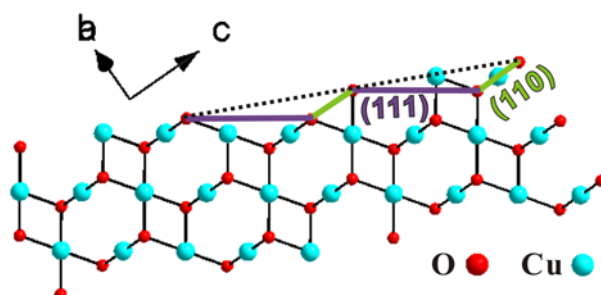


**Fig. S2** Schematic model of  $\text{Cu}_2\text{O}$  (332) surface projected along the  $[\bar{1}10]$  direction, showing that the (332) surface is a combination of 2(111) terraces (purple line)  $\times$  (110) monoatomic steps (green line).

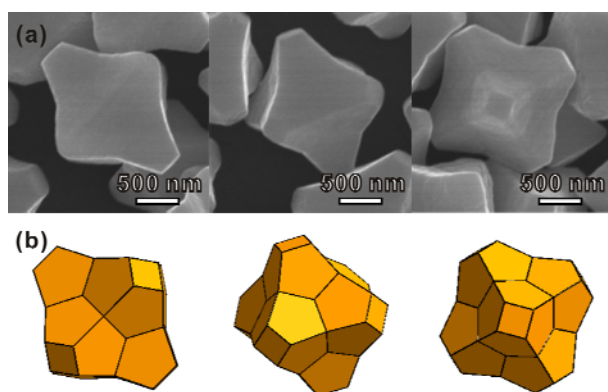


**Fig. S3** (a) High-magnification SEM images and (b) models of the truncated concave octahedral  $\text{Cu}_2\text{O}$  exposed with  $24\{332\}$  and six  $\{100\}$  facets, viewed from different directions.

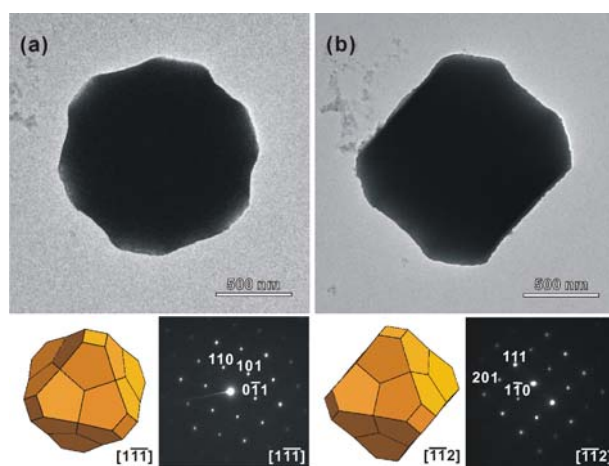


**Fig. S4** (a) Typical low-magnification TEM images, corresponding SAED patterns and schematic model of an ideal truncated concave octahedron with  $h:k:l$  to be  $1.08:1.08:1$ , viewed along the  $[\bar{1}\bar{1}\bar{1}]$  direction (c) and  $[\bar{1}\bar{1}2]$  direction (d) respectively.

Fig. S4a, 3b show the typical TEM images and corresponding SAED patterns of a truncated concave octahedron, and a proposed truncated concave octahedral model projected along different zone axes, respectively. The SAED patterns indicate that the as-prepared truncated concave octahedral  $\text{Cu}_2\text{O}$  microcrystals are single crystalline. In the proposed model, the facets in the apex of the concave octahedron are  $\{100\}$  facets and the planes of the concave trisoctahedron are expected to be  $\{hhl\}$  facets. To match the schematic model with the observed truncated concave octahedron, the  $h:h:l$  is inclined to  $1.08:1.08:1$ .

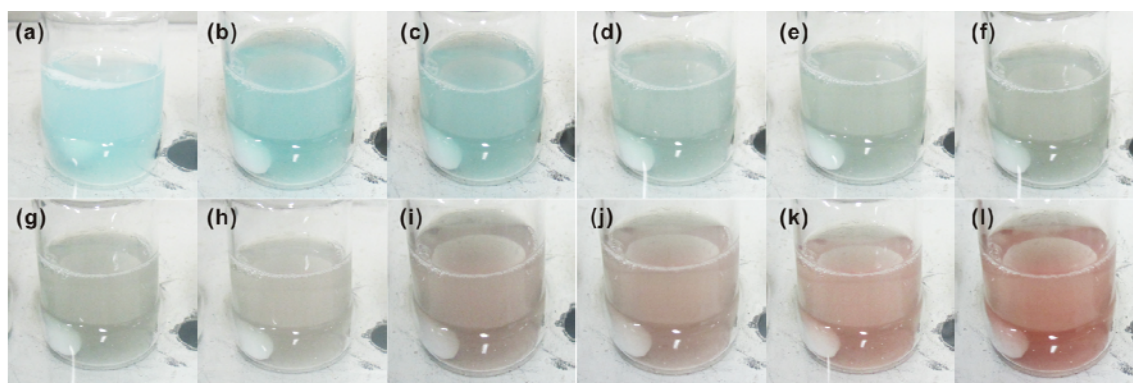


**Fig. S5** Photographs showing the change in the solution color as a function of reaction time in the synthesis of  $\text{Cu}_2\text{O}$  branched microcrystals in Figure 3a. (a) 30 s, (b) 210 s, (c) 240 s, (d) 330 s, (e) 420 s, (f) 480 s, (g) 540 s, (h) 11 min, (i) 14 min, (j) 15 min, (k) 17 min and (l) 19 min after adding glucose to start microcrystal growth.

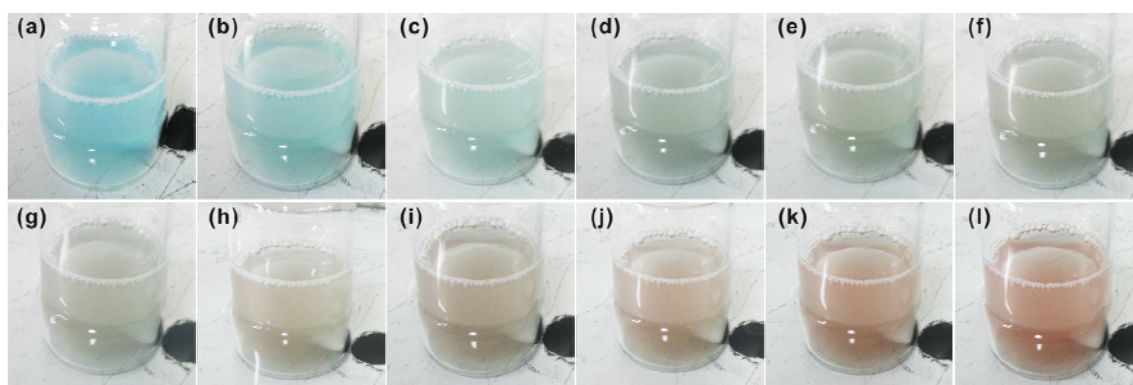


**Fig. S6** Photographs showing the change in the solution color as a function of reaction time in the synthesis of  $\text{Cu}_2\text{O}$  truncated concave octahedral microcrystals enclosed by  $24\{332\}$  and six  $\{100\}$  facets in Figure 3b. (a) 30 s, (b) 120 s, (c) 150 s, (d) 210 s, (e) 240 s, (f) 270 s, (g) 300 s, (h) 390 s, (i) 450 s, (j) 510 s, (k) 600 s and (l) 660 s after adding glucose to start microcrystal growth.

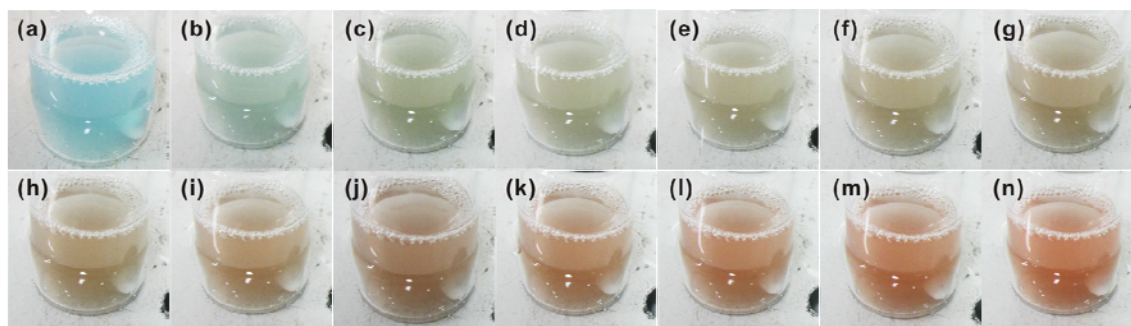


**Fig. S7** Photographs showing the change in the solution color as a function of reaction time in the synthesis of  $\text{Cu}_2\text{O}$  truncated concave octahedral microcrystals in Figure 3c which h: k: l is 1.08:1.08:1. (a) 30 s, (b) 90 s, (c) 150 s, (d) 180 s, (e) 210 s, (f) 240 s, (g) 270 s, (h) 300 s, (i) 330 s, (j) 360 s, (k) 390 s, (l) 420 s, (m) 450 s and (n) 480 s after adding glucose to start microcrystal growth.

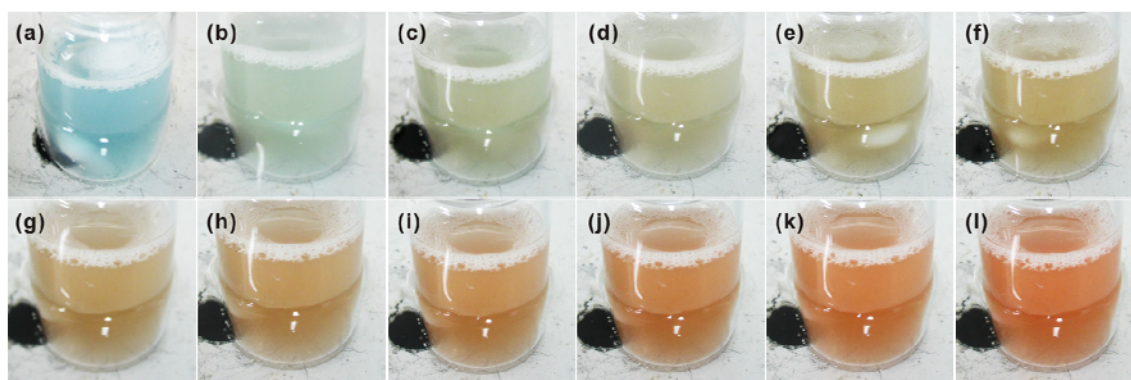


**Fig. S8** Photographs showing the change in the solution color as a function of reaction time in the synthesis of  $\text{Cu}_2\text{O}$  truncated octahedral microcrystals in Figure 3d. (a) 30 s, (b) 60 s, (c) 90 s, (d) 120 s, (e) 150 s, (f) 180 s, (g) 210 s, (h) 240 s, (i) 270 s, (j) 300 s, (k) 330 s and (l) 360 s after adding glucose to start microcrystal growth.

From the change in the solution color as a function of reaction time in the synthesis of  $\text{Cu}_2\text{O}$  shown in the Fig. S5-S8, we can conclude that the growth rate of  $\text{Cu}_2\text{O}$  increases with the increase of the concentration of glucose. As shown in Figure S5, in the synthesis of branched structure  $\text{Cu}_2\text{O}$  with 2 mM glucose, the solution color is still blue after 330s of reaction (Fig. S5d), and become light brick-red until 11 min (660 s) of reaction (Fig. S5h). Then brick-red in the solution becomes deeper and deeper (Fig. S5i-S5l). When the concentration of glucose increased to 5 mM, the solution color is light green after 210 s of reaction (Fig. S6d) and become light brick-red after 390s of reaction (Fig. S6h), and then the brick-red is also deeper and deeper (Fig. S6i-S6l). However, the growth rate

became fast when the concentration of glucose is 8 mM. As shown in Figure S7, the solution color became light green after 90 s of reaction (Fig. S7b), and light brick-red after 150 s of reaction (Fig. S7c). When the concentration of glucose increased to 16 mM, the growth rate is much faster (Fig. S8). The solution color is green after 60 s of reaction (Fig. S8b), and become brick-red after 90 s of reaction (Fig. S8c).

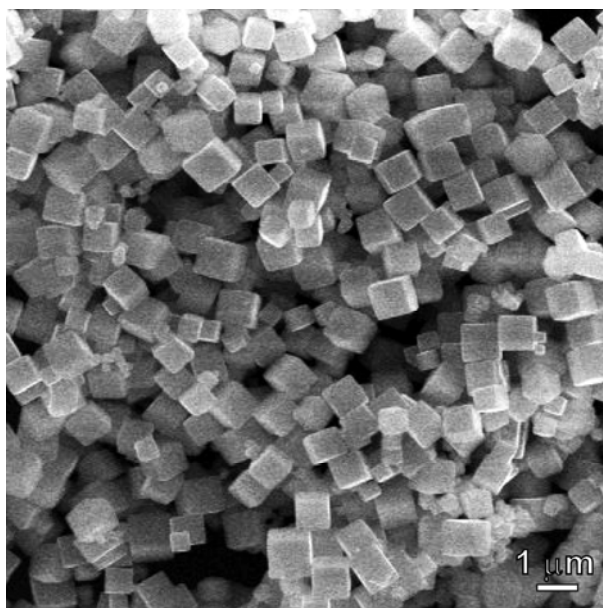


**Fig. S9** The SEM image of cubic Cu<sub>2</sub>O microcrystals.

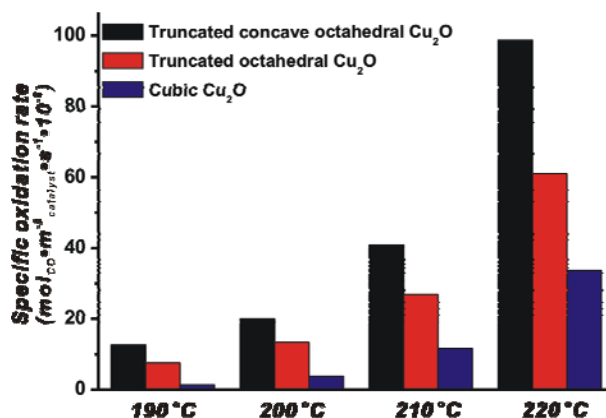


**Fig. S10** Specific oxidation rates of CO over Cu<sub>2</sub>O microcrystals with different morphologies at different temperatures.

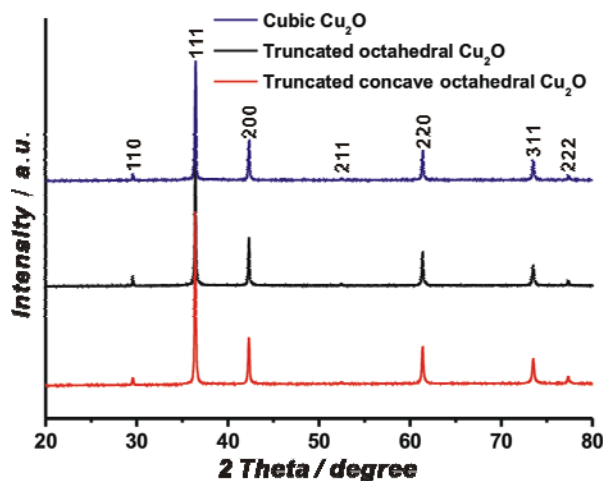


**Fig. S11** XRD patterns of  $\text{Cu}_2\text{O}$  microcrystals obtained after catalytic CO oxidation up to 220 °C.

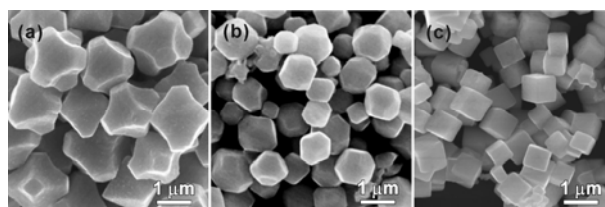


**Fig. S12** SEM images of  $\text{Cu}_2\text{O}$  microcrystals obtained after catalytic CO oxidation up to 220 °C: (a) truncated concave octahedral  $\text{Cu}_2\text{O}$ , (b) truncated octahedral  $\text{Cu}_2\text{O}$  and (c) cubic  $\text{Cu}_2\text{O}$ .

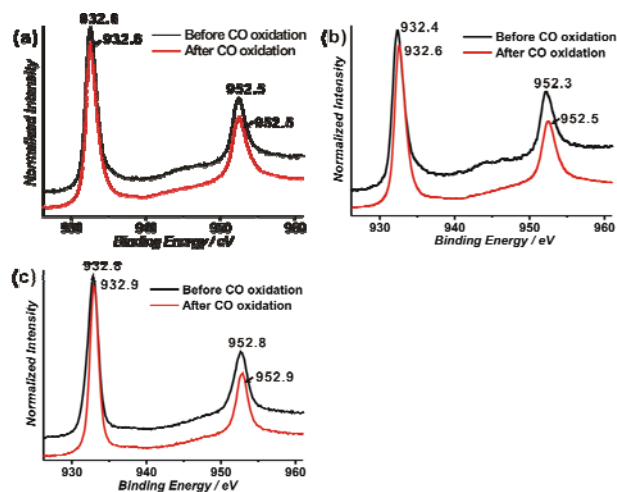


**Fig. S13** XPS results of  $\text{Cu}2p$  of  $\text{Cu}_2\text{O}$  microcrystals before and after catalytic CO oxidation: (a) truncated concave octahedral  $\text{Cu}_2\text{O}$  microcrystals, (b) truncated octahedral  $\text{Cu}_2\text{O}$  microcrystals and (c) cubic  $\text{Cu}_2\text{O}$  microcrystals.